Synchronization engineering: Theoretical framework and application to dynamical clustering

Hiroshi Kori,[1,a)] Craig G. Rusin,[2] István Z. Kiss,[3] and John L. Hudson[2]
[1]*Department of Mathematics, Hokkaido University, Sapporo, Hokkaido, 060-0810, Japan*
[2]*Department of Chemical Engineering, University of Virginia, Charlottesville, Virginia 22904-4741, USA*
[3]*Department of Chemistry, Saint Louis University, St. Louis, Missouri 63103, USA*

(Received 9 January 2008; accepted 23 April 2008; published online 27 June 2008)

A method for engineering the global behavior of populations of rhythmic elements is presented. The framework, which is based on phase models, allows a nonlinear time-delayed global feedback signal to be constructed which produces an interaction function corresponding to the desired behavior of the system. It is shown theoretically and confirmed in numerical simulations that a polynomial, delayed feedback is a versatile tool to tune synchronization patterns. Dynamical states consisting of one to four clusters were engineered to demonstrate the application of synchronization engineering in an experimental electrochemical system. © *2008 American Institute of Physics*.
[DOI: 10.1063/1.2927531]

Populations of interacting rhythmic components can produce complex behavior in biology,[1,2] communications,[3] population dynamics,[4] and chemistry.[5–8] In biology, synchronization can be beneficial, such as in orchestrating the circadian rhythms in mammals, or pathological, such as in the occurrence of Parkinson's disease. We consider here the engineering of desirable states through the introduction of mild feedback, mild such that the behavior of the individual components is not substantially changed by the introduction of the external signal. In a previous paper,[9] we have experimentally demonstrated a general methodology for engineering a target dynamical behavior in oscillator assemblies. The aim of the present paper is to describe the theory behind our methodology and to verify it by numerical and experimental studies.

I. INTRODUCTION

Ensembles of self-sustained oscillators can spontaneously organize their collective dynamical behavior as a result of interaction among elements. Examples can be found in biological,[1,2] chemical,[5–8] and ecological systems,[4] communications,[3] as well as human activities.[10] Global behaviors such as synchronization are often responsible for the formation of certain beneficial biological functions, such as, orchestrating the sleep/wake cycle (circadian rhythm) of mammals.[11] Conversely, pathological synchronization may induce serious problems, e.g., tremors in Parkinson's disease[2] and abnormal sway in London's Millennium Bridge.[12]

Interactions involving feedback among rhythmic elements are often associated with the formation of dynamical order. In many cases, feedback plays an essential role in sustaining dynamical stability and in suppressing complexity. In chemical systems, several types of complex synchronized behavior emerge by introducing global feedback, which otherwise shows simple synchronization or chemical turbulence.[8,13,14] It may be expected that feedback loops among neuronal clusters contribute to the design of the complex dynamical functionality of the brain.[15] In medical applications, heart pacemakers, deep brain pacemakers, and feedback control techniques have been proposed to eliminate pathological synchronization.[2,16] For applications which involve biological neurons, a mild control is desired to avoid side effects and to maintain the fundamental nature of neurons in the system.

In this paper we present a comprehensive theory for designing the collective dynamics of a rhythmic population using external feedback and, as an application of its use, demonstrate the power of the methodology for creating various cluster states in both numerical simulations and experimental studies.

This method has been shown to be extremely robust in engineering collective dynamical behavior in electrochemical experiments.[9] Our method utilizes phase modeling[5] (as opposed to a physiochemical modeling) to describe the dynamical behavior of rhythmic elements. The simplicity and analytical tractability of the phase model is exploited to design an optimal, delayed, nonlinear feedback signal for obtaining a desired collective behavior. The only properties required to construct the phase model are the waveform and the phase response function of the oscillator, which can be experimentally measured. Section II outlines the mathematics of the methodology. In Sec. III, the detailed description of the feedback design method is presented, which is further developed in Sec. IV for both harmonic and slightly inharmonic waveforms. Sections V and VI present examples of synchronization engineering using numerical studies via the Brusselator model and experimental studies using electrochemical oscillators, respectively.

[a)]Present address: Division of Advanced Sciences, Ochadai Academic Production, Ochanomizu University, Tokyo, 112-8610, Japan. Electronic mail: kori.hiroshi@ocha.ac.jp.

 © 2008 American Institute of Physics

Author complimentary copy. Redistribution subject to AIP license or copyright, see http://cha.aip.org/cha/copyright.jsp

II. GENERAL METHODOLOGY

Our methodology seeks to engineer a target collective dynamical behavior into a population of limit-cycle oscillators through feedback. A phase model is used to describe the collective behavior of a population of weakly coupled oscillators. For N oscillators with general interactions (which also admits interactions through a complex network), the phase model is given as

$$\frac{d\phi_i}{dt} = \omega_i + K\sum_j H_{ij}(\phi_j - \phi_i), \tag{1}$$

where ϕ_i $(0 \leqslant \phi_i < 2\pi)$ and ω_i are the phase and the natural frequency of the oscillator i, K is a coupling strength $(K>0)$, and the 2π periodic function $H_{ij}(\phi)$ is the (phase) interaction function (or, phase coupling function). The phase model is derived as the first order approximation of a coupled limit-cycle oscillator system, where the small quantity is the coupling intensity K.[5] The interaction function $H_{ij}(\phi)$ can be calculated from the properties of the limit-cycle oscillator i and physical interaction from the oscillator j to the oscillator i. The details of this derivation are presented in Sec. III. Although, as presented in Sec. III, our proposed theory may deal with Eq. (1), we mostly devote ourselves in the present paper to the case of global feedback. In such a case, the phase model is reduced to

$$\frac{d\phi_i}{dt} = \omega_i + \frac{K}{N}\sum_j H_i(\phi_j - \phi_i). \tag{2}$$

Moreover, if the heterogeneity is sufficiently small compared to the feedback intensity K, we can treat the system as identical oscillators. In such a case, we may use the following phase model:

$$\frac{d\phi_i}{dt} = \omega + \frac{K}{N}\sum_j H(\phi_j - \phi_i). \tag{3}$$

For simplicity, we outline our methodology in terms of Eq. (3) in this section.

In the phase model (3), dynamical evolution of the system is predicted if the interaction function $H(\phi)$ and an initial condition are given. This comes from the fact that we may set $\omega=0$ and $K=1$ without loss of generality (using a rotating reference frame, $\phi-\omega t \to \phi$, and rescaling time, $Kt \to t$). The relationship between the shape of the interaction function and the global dynamical behavior of the system has been well studied. For example, the conditions which admit perfect synchrony, perfect desynchrony (the spray state),[5] phase clustering,[17] and slow switching dynamics[18–20] are known. While it is possible for an interaction function to admit multiple attractors, it is preferable to have a single stable attractor (or at least a single dominant basin of attraction). If a coupled limit-cycle oscillator system has a phase interaction function which results in a single stable attractor, the system should exhibit the expected global behavior under general initial conditions.

Two steps are required to engineer a desired target behavior:

(i) Find an interaction function $H(\phi)$ which uniquely stabilizes the desired collective behavior;
(ii) Seek the physical feedback parameters which result in the interaction function found in (i).

The difficulty of step (i) depends on the desired target behavior. To illustrate the engineering methodology, we have selected a simple collective behavior which has been well characterized in terms of the phase model: perfect synchrony and balanced cluster states. Two different approaches can be utilized to optimize feedback parameters. The first approach simply requires knowledge of the *precise* interaction function to be targeted. However, there are many cases (such as phase clustering) in which there exists a large family of valid functions, each capable of producing the desired target behavior. By arbitrarily selecting one of these functions, the most effective means of generating the target behavior may be overlooked. Additionally, an arbitrary choice of an interaction function can substantially increase the difficulty of the feedback parameter optimization. Therefore, instead of targeting a precise interaction function, we place constraints on specific properties of the interaction function as required to generate the appropriate behavior. The optimum feedback parameters are selected such that the associated interaction function meets these constraints with the minimum feedback amplitude.

To engineer a target interaction function into a physical system, we introduce a feedback $Kp(t)$ to some global parameter of the system with the following functional form:

$$p(t) = \frac{1}{N}\sum_{i=1}^{N} h(x_i), \tag{4}$$

$$h(x_i) = \sum_{n=0}^{S} k_n[x_i(t-\tau_n) - a_0]^n, \tag{5}$$

where $x_i(t)$ is an observable variable of the oscillator i at time t, a_0 is the time average of x_i, k_n and τ_n the gain and the delay of the nth order feedback respectively, and K and S the overall gain and the overall order of the feedback, respectively. Our choice of function (5) is motivated from the fact that each feedback term yields different combinations of intensities of Fourier components and the feedback delay value τ_n controls the ratio between the symmetric and antisymmetric Fourier components. In addition, the nth harmonic of the interaction function is efficiently enhanced by the nth order feedback. Thus, flexible and efficient design of the interaction function is possible. In Sec. III, we show that any target interaction function which is composed of Sth and lower Fourier components can be indeed produced by using the S overall order feedback. In particular, when the waveform $x_i(t)$ is exactly harmonic, feedback parameter values $\{k_n\}$ and $\{\tau_n\}$ may be calculated analytically, as illustrated in Sec. IV. For a general waveform, a numerical optimization is often required to determine the feedback parameters.

III. THEORY OF FEEDBACK DESIGN

We present a theory for designing the external feedback signal yielding a desired phase interaction function. Because

Author complimentary copy. Redistribution subject to AIP license or copyright, see http://cha.aip.org/cha/copyright.jsp

the extension to more complex situations is straightforward, it is suitable to start with the case where the oscillator 1 is affected by the feedback signal composed as a function of the state variable of the oscillator 2. The dynamical equation for the oscillator 1 is then given as

$$\frac{d\boldsymbol{A}_1(t)}{dt} = \boldsymbol{F}_1[\boldsymbol{A}_1(t)] + K\boldsymbol{P}(t), \tag{6}$$

where $\boldsymbol{A}_i=(x_i,y_i,\ldots)^T$ is the state variable of the oscillator $i(i=1,2)$, $\boldsymbol{F}_i(\boldsymbol{A}_i)$ is a nonlinear function admitting limit-cycle oscillation, and $\boldsymbol{P}(t)$ is a feedback signal. The dynamical equation for the oscillator 2 is arbitrary provided that it produces nearly periodic dynamics. We define the observable variable to be x and the variable to be perturbed by the feedback to be y (these variables need not be mutually exclusive, which is the case in the numerical studies and experiments). Thus,

$$\boldsymbol{P}(t) = \{0,h(x_2),0,\ldots,0\}^T, \tag{7}$$

where $h(x)$ is Eq. (5).

Because we are interested in mild engineering, we assume that the overall gain K is small such that the dynamical behavior of the system Eq. (6) can be approximated by the phase oscillator model,

$$\frac{d\phi_1}{dt} = \omega_1 + KH(\phi_2-\phi_1). \tag{8}$$

The interaction function $H(\phi_2-\phi_1)$ is computed as

$$H(\phi_2-\phi_1) = \frac{1}{2\pi}\int_0^{2\pi} Z(\phi_1+\theta)h(\phi_2+\theta)d\theta, \tag{9}$$

where $Z(\phi_1)$ and $h(\phi_2)$ are evaluated from single isolated oscillators 1 and 2, respectively. The function $Z(\phi_1)$ is referred to as the phase response function (or, the phase sensitivity function) of the oscillator 1, which is the gradient of the phase along the y-direction on the limit-cycle orbit $\boldsymbol{A}_1^C(\phi)$,

$$Z(\phi_1) = \left.\frac{\partial\phi_1}{\partial y_1}\right|_{\boldsymbol{A}_1=\boldsymbol{A}_1^C}. \tag{10}$$

There are several ways to measure $Z(\phi)$ of a given oscillator. (For example, see Ref. 5 for the analytical derivation, the software by Ermentrout, xppaut, for the numerical derivation, and Refs. 21–23 for the experimental derivation. Some of the methods are reviewed in Ref. 24.) The function $h(\phi_2)$ is obtained by first describing $x_2(t)$ as the function of the phase of the oscillator, $x_2(\phi_2)$. Because $\phi_2(t-\tau)=\phi_2(t)-\omega_2\tau$ when the interaction is absent, we have $x_2[\phi_2(t-\tau)]=x_2[\phi_2(t)-\omega_2\tau]$. As a result, $h(\phi_2)$ assumes the form

$$h(\phi_2) = \sum_{n=0}^{S} k_n[x(\phi_2-\omega_2\tau_n)-a_0]^n, \tag{11}$$

or, upon expanding $x(\phi)=\Sigma_l a_l e^{-il\phi}$, as

$$h(\phi_2) = \sum_{n=0}^{S} k_n\left(\sum_{l\neq 0} a_l e^{-il\phi_2}e^{il\omega_2\tau_n}\right)^n. \tag{12}$$

Thus, the phase model is an autonomous system despite the existence of time delays in the original system (6). Such an approximation is valid so long as $K\tau$ remains small (note that the dimension of K is inverse time).[19,25]

For given $Z(\phi_2)$, the feedback parameters k_n and τ_n yielding a target $H(\phi)$ are found in the following way. To simplify the problem, the functions are expanded into their Fourier series, $H(\phi)=\Sigma_l H_l e^{-il\phi}$, $Z(\phi)=\Sigma_l Z_l e^{-il\phi}$, and $h(\phi)=\Sigma_l h_l e^{-il\phi}$ (where $H_l=H_{-l}^*, Z_l=Z_{-l}^*$, and $h_l=h_{-l}^*$). Using these Fourier coefficients, we obtain the relation

$$H_l = h_l Z_{-l}, \tag{13}$$

where h_l is the function of k_n and τ_n. By solving a set of complex equations (13), the feedback parameters k_n and τ_n can be determined. In theory, any interaction function composed of harmonic components H_l for $0\leqslant l\leqslant S$ can be constructed using a feedback signal with an overall order of S, provided that z_l for $l=0,\ldots,S$ is nonvanishing.

It is important to point out that the flexibility of our engineering method is reduced for certain types of oscillators. For example, the Stuart–Landau oscillator (i.e., the normal form for the Hopf bifurcation) has $Z_l=0$ for $l\geqslant 2$,[5] forcing all higher harmonics ($l\geqslant 2$) in the interaction function to vanish regardless of the nonlinear terms in the feedback. A similar problem may occur in systems which contain special symmetry. For example, the Van der Pol oscillator has symmetry with respect to the center of the oscillation. This fact implies that $Z(\phi+\pi)=Z(\phi)$, i.e., $Z_l=0$ for even l. Thus, the even Fourier components of the interaction function vanish. In these special cases, the methodology is limited to controlling only those harmonics of the $H(\phi)$ which do not correspond to the vanishing harmonics in $Z(\phi)$.

It is straightforward to extend the above arguments to a population of oscillators. Under the assumption that a parameter in each individual oscillator can be independently tuned online, we may consider

$$\frac{d\boldsymbol{A}_i(t)}{dt} = \boldsymbol{F}_i[\boldsymbol{A}_i(t)] + K(0,p_i,\ldots)^T, \tag{14}$$

where the function p_i is fully generalized as

$$p_i(t) = \sum_j \sum_{n=0}^{S} k_{ij}^{(n)} y_j^n[t-\tau_{ij}^{(n)}]. \tag{15}$$

The corresponding phase model then reads Eq. (1). The interaction function $H_{ij}(\phi)$ is determined as a function of the physical feedback parameters $[k_{ij}^{(n)}]$ and $[\tau_{ij}^{(n)}]$; any $H_{ij}(\phi)$ can be designed by giving appropriate feedback parameters. The phase model (1) is very general and a large class of collective behavior can be engineered.

A simple situation, which is the case in the numerical and experimental studies in Secs. V and VI, is that a global parameter of the system is tuned by feedback. In such a case, we consider the phase model (3) by adopting the global feedback signal Eqs. (4) and (5).

Author complimentary copy. Redistribution subject to AIP license or copyright, see http://cha.aip.org/cha/copyright.jsp

IV. USE OF HARMONIC SIGNALS

An oscillator may appear to have a nearly harmonic waveform by the nature of oscillation or through the use of a low pass filter. In the case of a perfectly harmonic waveform, feedback parameters can be explicitly calculated and the effect of each feedback term on the interaction function clearly understood. However, it is unrealistic to assume that an exact harmonic waveform can be obtained experimentally. Therefore, the effect of a weakly inharmonic waveform is also examined.

A. Harmonic waveform

We first assume that $x(\phi)$ is an exact harmonic waveform with zero mean. Properly defining the origin of the phase, we may set

$$x(\phi) = e^{-i\phi} + \text{c.c.}, \tag{16}$$

where c.c. indicates the complex conjugate (i.e., $e^{i\phi}$ in this case).

Introducing $\phi_n \equiv \phi - \omega\tau_n$, we obtain

$$x(\phi_n)^n = \sum_{m=0}^{n} C_m^n e^{i(n-2m)\phi_n}, \tag{17}$$

where C_m^n is a number of m combinations from a set of n elements. Since $x(\phi_n)^n$ contains only lth harmonics (where $l=n,n-2,n-4,\ldots$) the nth feedback term in Eq. (13) only contributes to the lth ($l=n,n-2,n-4,\ldots$) Fourier components of the interaction function. The feedback delay varies the ratio between the even and odd components of each harmonic.

Combining the feedback terms using Eq. (5) yields an interaction function composed of Fourier components H_l for $l \leqslant S$,

$$h(\phi) = \sum_{n=0}^{S} \sum_{m=0}^{n} C_m^n e^{i(n-2m)\phi_n} \tag{18}$$

or, for $l \geqslant 0$,

$$h_l = \sum_{n=l}^{S} k_n C_{n+l/2}^n e^{il\omega\tau_n}, \tag{19}$$

where for convenience we define $C_m^n = 0$ if m is not an integer. Therefore,

$$H(\phi) = \sum_{n=0}^{S} k_n \sum_{m=0}^{n} C_m^n z_{n-2m} e^{i(2m-n)\phi_n}, \tag{20}$$

or, for $l \geqslant 0$,

$$H_l = z_{-l} \sum_{n=l}^{S} k_n C_{n+l/2}^n e^{il\omega\tau_n}. \tag{21}$$

Therefore, for a given target H_l, ($l=0,\ldots,S$), the feedback parameters k_n and τ_n ($n=0,\ldots,S$) can be explicitly obtained. Since H_S is determined solely by the Sth term, the parameters k_S and τ_S can be found by solving a complex equation obtained by setting $l=S$. The same process can be used for the H_{S-1} component, to solve for the parameters k_{S-1} and τ_{S-1}. Since H_{S-2} is dependent on the Sth and $(S-2)$th terms, k_{S-2} and τ_{S-2} can be determined. Repeating this processes for each term, all feedback parameters can be calculated.

As an illustration, the feedback parameters required to produce a Hansel–Manubille–Mato-type[18] interaction function will be calculated. The target function $H(\phi)$ is selected to be

$$H(\phi) = \sin(\phi - \alpha) - r\sin(2\phi) = -\frac{i}{2}e^{i\alpha}e^{-i\phi} + \frac{ir}{2}e^{-2i\phi} + \text{c.c.}, \tag{22}$$

where α and $r>0$ are the parameters of the function. Since the target interaction function has second order components, second order feedback is required. Therefore, Eq. (20) for $S=2$ becomes

$$H(\phi) = (k_0 + 2k_2)z_0 + k_1 z_{-1} e^{i\omega\tau_1} e^{-i\phi} + k_2 z_{-2} e^{2i\omega\tau_2} e^{-2i\phi} + \text{c.c.} \tag{23}$$

Comparing Eqs. (22) and (23), we find one of the solutions to be

$$k_0 = -\frac{r}{|z_{-2}|}, \quad k_1 = \frac{1}{2|z_{-1}|}, \quad k_2 = \frac{r}{2|z_{-2}|}, \tag{24}$$

$$\tau_1 = \frac{\alpha - \frac{\pi}{2} - \arg(z_{-1})}{\omega}, \quad \tau_2 = \frac{\frac{\pi}{2} - \arg(z_{-2})}{2\omega}. \tag{25}$$

B. Slightly inharmonic waveform

The effect of weak inharmonic components is considered using the waveform

$$x(\phi) = e^{i\phi} + \epsilon e^{i2\phi} + O(\epsilon^2) + \text{c.c.}, \tag{26}$$

where ϵ is a small complex number. Introducing $\phi_n = \phi - \omega\tau_n$, for $n \geqslant 1$ yields

$$x(\phi_n)^n = \sum_{m=0}^{n} C_m^n e^{i(n-2m)\phi_n} + \epsilon \sum_{m=0}^{n-1} C_m^{n-1}[e^{i(n-2m+1)\phi_n} + e^{i(n-2m-3)\phi_n}] + O(\epsilon^2), \tag{27}$$

and $x^0=1$. The nth term contributes to the lth ($l=n+1, n-1,\ldots$) harmonic with order ϵ. Sth order feedback strongly enhances the harmonics h_l of the interaction function for $l \leqslant S$. Therefore, Sth order feedback is required to produce a target interaction function composed of harmonics $l \leqslant S$. Although the $(S+1)$th Fourier component appears in the interaction function, it is expected to be very small [of the order of $O(\epsilon Z_{S+1})$] and can be safely neglected. Similarly, this result is also true in cases where the first order Fourier component of the waveform is dominant.

When the waveform is strongly inharmonic, each feedback term enhances various harmonics, including higher order harmonics H_l ($l>S$) of the interaction function. In these situations, no analytical solution is possible, and the feedback parameters must be numerically optimized using

Author complimentary copy. Redistribution subject to AIP license or copyright, see http://cha.aip.org/cha/copyright.jsp

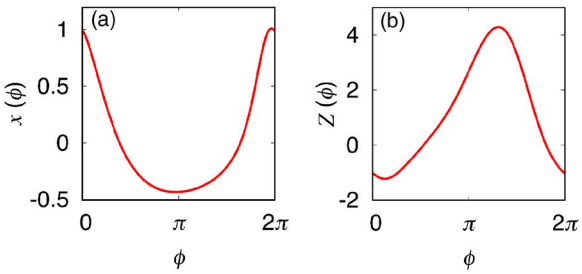

FIG. 1. (Color online) Waveform $x(\phi)$ and phase response function $Z(\phi)$ of the Brusselator oscillator. The parameter values are $A=1.0$ and $B=2.3$, resulting in $T=6.43$ and $\omega=0.977$.

Eq. (9) or Eq. (13). In addition, usually, a high order feedback is required (i.e., large S) such that Z_l for $l>S$ are negligible.

V. NUMERICAL STUDY: PHASE CLUSTERING

Our methodology is numerically verified for a population of limit-cycle oscillators, using the Brusselator model, a simple two variable ODE system that admits a Hopf bifurcation.[26] The dynamical equations for a Brusselator population under global feedback are

$$\frac{dx_i}{dt} = (B-1)x_i + A^2 x_i + f(x_i,y_i) + \frac{K}{N}\sum_{j=1}^{N} h(x_j),$$
$$\frac{dy_i}{dt} = -Bx_i - A^2 y_i - f(x_i,y_i), \tag{28}$$

where $f(x,y)=(B/A)x^2+2Axy+x^2y$. Here, it is assumed that the feedback signal is constructed from and applied to the variables x_i. Note that for convenience, the variables x_i and y_i are transformed such that the fixed point is shifted to $(x,y)=(0,0)$. For a single uncoupled oscillator, the Hopf bifurcation occurs at $B=B_c\equiv 1+A^2$. The parameters of Eq. (28) were chosen to be $A=1.0$ (so that $B_c=2.0$) and $B=2.3$. The waveform $x(\phi)$ and the response functions $Z(\phi)$ along the x-direction (the response function is calculated using xppaut) are displayed in Fig. 1, and their Fourier coefficients can be found in Table I.

The phase of an oscillator ϕ_i is determined by measuring the times at which the orbit in (x_i,y_i) state space crosses a particular point on its limit cycle. The phase of the oscillator $\phi_i(t)$ for $t_{m-1}\leqslant t<t_m$ can be defined as

TABLE I. Brusselator ($A=1,B=2.3$). Fourier coefficients of the wave form $x(\phi)$ and the phase response function $Z(\phi)$.

l	0	1	2	3	4	5
Re a_l	0.00	0.30	0.12	0.05	0.02	0.00
Im a_l	⋯	0.00	0.00	−0.01	−0.01	−0.01
$\lvert a_l\rvert$	0.00	0.30	0.12	0.05	0.02	0.01
Re Z_l	1.19	−0.98	−0.20	0.04	0.01	0.00
Im Z_l	⋯	−0.85	0.21	0.01	−0.01	−0.00
$\lvert Z_l\rvert$	1.19	1.29	0.28	0.04	0.01	0.00

$$\phi_i(t) = \frac{2\pi(t-t_{m-1})}{t_m - t_{m-1}}, \tag{29}$$

where t_m is defined as the time at which the mth crossing occurs. Note that $0\leqslant\phi_i(t)<2\pi$. To quantify the amount of collective global order within the system, it is useful to introduce the order parameter R_k,

$$R_k = \left|\frac{1}{N}\sum_{j=1}^{N} e^{ik\phi_j}\right|. \tag{30}$$

For a large population (i.e., large N), $R_k=0$ for uniform phase distribution and $R_k=1$ for a balanced k cluster state, in which the population is split into k equally populated point clusters distributed uniformly in phase (see the Appendix).

Phase clustering commonly appears in globally coupled oscillator systems.[17,27] In systems of identical coupled oscillators, these states always exist independent of the interaction function, such that the only outstanding issues to be addressed are the stability and the basin of attraction of the states. In this example, four parameter sets are created [one for each cluster state $(n=1,2,3,4)$] with the following conditions:

(i) the n cluster state is uniquely stable among the balanced cluster states;
(ii) the cluster state has high linear stability;
(iii) small amplitude feedback is preferable.

For condition (i), it is convenient to use a target interaction function of the form $\mathrm{Im}\,H_n>0$ and $\mathrm{Im}\,H_l\leqslant 0$ for $l\neq n$ (note that the symmetric parts $\mathrm{Re}\,H_l$ are irrelevant to the stability of the balanced cluster states, so that we may arbitrarily set the symmetric parts). For such an interaction function, the maximum eigenvalue is given by $\lambda_{\max}^{(n)}=-\Sigma_{l=1}^{\infty}2l\,\mathrm{Im}\,H_{nl}$ (see the Appendix for the details). We thus require $\lambda_{\max}^{(n)}<0$. Satisfying condition (ii) requires that $\mathrm{Im}\,H_n$ is large enough for high stability. To satisfy condition (iii), nth order feedback is used to generate the nth cluster state (i.e., $S=n$), since the nth cluster state requires nth order harmonics in its interaction function.

A large number of interaction functions satisfies conditions (i) and (ii). Out of this family of interaction functions, the optimal feedback parameter set is selected such that it minimizes the cost function $\Sigma_{l=1}^{n}|k_l|$ under the conditions shown in the left side of each column of Table II. The table also displays the optimized feedback parameter sets (obtained numerically using Mathematica), the resulting $\mathrm{Im}\,H_l$ (in the right side of each column), and the resulting maximum eigenvalue $\lambda_{\max}^{(n)}$.

Applying the optimized feedback parameter sets to Eq. (28) causes the system to approach the desired cluster states. The convergence of the system to the cluster states is illustrated in Fig. 2, using the appropriate order parameter R_n. Several different random initial conditions were used for each parameter set and in each case the desired cluster state was obtained (not shown).

It is worth noting that, in practice, the 3 and 4 cluster states are difficult to obtain unless high order feedback is used. For example, when only the linear term is used, the

Author complimentary copy. Redistribution subject to AIP license or copyright, see http://cha.aip.org/cha/copyright.jsp

TABLE II. Brusselator population with global feedback. The target and resulting interaction functions, feedback parameters, and the resulting maximum eigenvalue for the n cluster state.

n	1		2		3		4	
$\mathrm{Im}\,H_1$	>1.0	1.00	<-1.0	−1.00	<-1.0	−3.28	<-1.0	−9.04
$\mathrm{Im}\,H_2$	<0.0	−0.07	>0.3	0.30	<-0.4	−0.40	<-0.4	−3.27
$\mathrm{Im}\,H_3$	<0.0	−0.01	<0.0	−0.00	>0.2	0.20	<-0.2	−0.20
$\mathrm{Im}\,H_4$	<0.0	−0.00	<0.0	−0.00	<0.0	−0.02	>0.15	0.15
k_1 τ_1	−2.56	2.40	2.01	2.06	0	0	0	0
k_2 τ_2	⋯	⋯	−6.50	0.44	35.7	2.95	0.25	5.26
k_3 τ_3	⋯	⋯	⋯	⋯	19.3	0.68	68.6	3.61
k_4 τ_4		⋯	⋯	⋯	⋯	⋯	42.0	0.32
$\lambda_{\max}^{(n)}$	−1.72		−1.16		−1.18		−0.80	

magnitude $|H_l|=|Z_l a_l|$ is very small for $l\geqslant 3$. This fact implies that the maximum eigenvalue of the $n\geqslant 3$ cluster states cannot be large and negative. Therefore, the presence of noise or heterogeneity, if any, would destroy the $n\geqslant 3$ cluster states.

VI. EXPERIMENTAL STUDIES

A. Experimental setup

The preceding theoretical work on synchronization engineering was experimentally tested using a population of electrochemical oscillators. These oscillators were created using an electrochemical cell which consisted of 64 Ni electrodes (99.99% pure) in a 3 M H_2SO_4 solution, a Pt mesh counter electrode, and a $Hg/Hg_2SO_4/K_2SO_4$ (sat) reference electrode. The cell was enclosed in a jacketed glass vessel held at a constant temperature of 11 °C. An EG&G potentiostat was used to adjust the circuit potential (V) of the cell, causing the nickel electrodes to undergo transpassive dissolution. The dissolution current of each electrode, $I_j(t)$, was measured by zero resistance ammeters (ZRA). A resistor (R_p) was at-

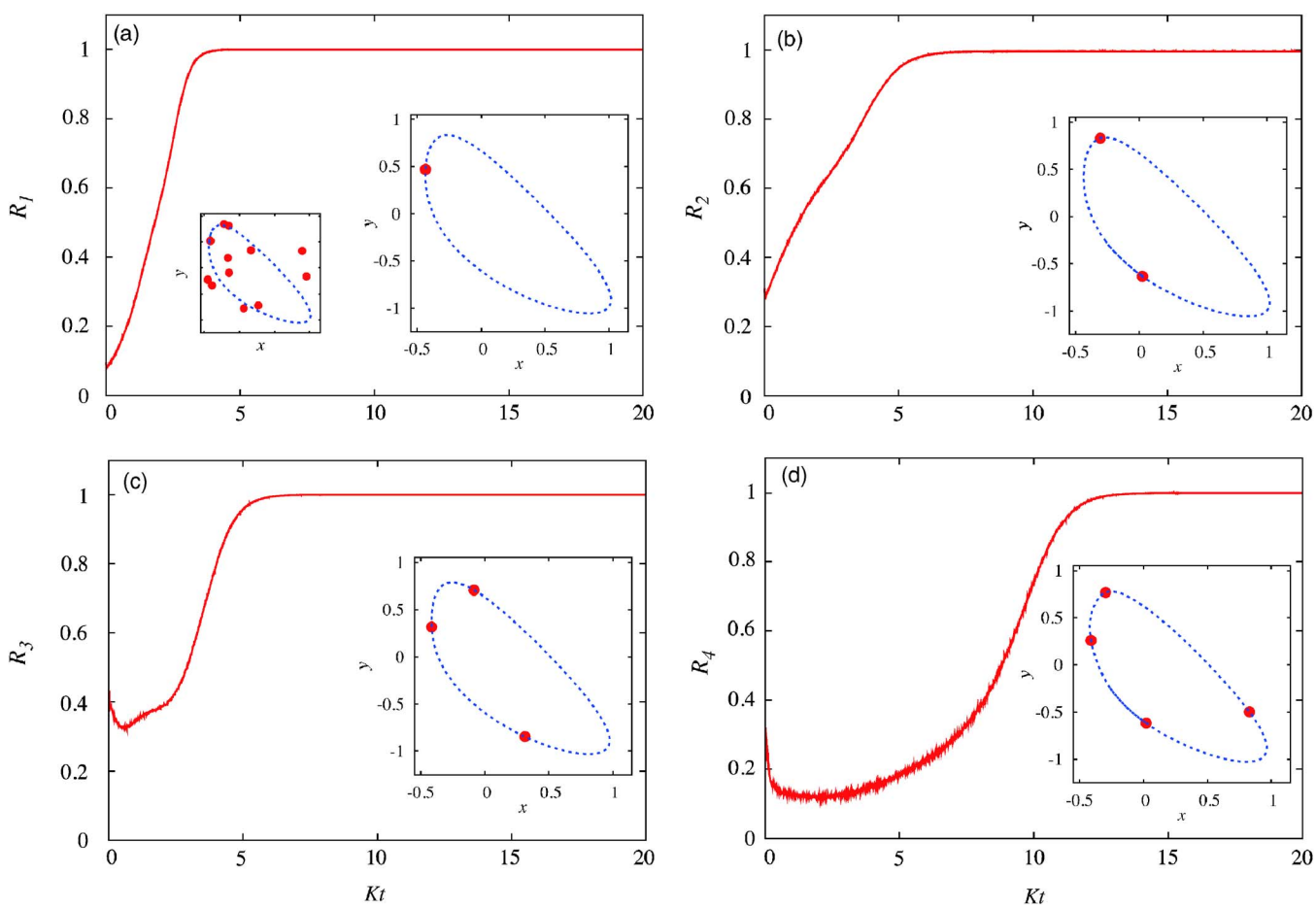

FIG. 2. (Color online) Engineering cluster states in the Brusselator model. Time traces of the order parameters R_n and snapshots for (a) $n=1$, (b) $n=2$, (c) $n=3$, and (d) $n=4$ for $N=12$ and $K=0.001$. In each panel, the parameter set n displayed in Table II is used. In the insets, snapshots in the one-oscillator phase space at $Kt=20$ are displayed. The dashed lines are the orbits of an oscillator. In panel (a), initial conditions are shown (on the left side). Note that the initial condition is the same for all panels.

Author complimentary copy. Redistribution subject to AIP license or copyright, see http://cha.aip.org/cha/copyright.jsp

tached to each channel to induce oscillations in the electrode potential. A Labview based real time data acquisition computer was used to read the ZRA measurements, stream these measurements to the host machine, and apply the feedback signal to the potentiostat at a rate of 250 Hz. The current measurements were scaled:

$$I_j'(t) = \frac{A_{\text{mean}}}{A_j}[I_j(t) - I_j^{\text{offset}}]. \tag{31}$$

The mean value of each channel (I_j^{offset}) was removed from the measurement, and the result was scaled by the amplitude of its oscillation (A_j) relative to the mean amplitude of the population (A_{mean}). The host machine was used to continuously determine the offset and amplitude of each rhythmic element in the population. To calculate the feedback signal, the potential drop across the double layer, $x_j(t)$, was determined from the scaled current measurements

$$x_j(t) = V(t) - I_j'(t)R_p, \tag{32}$$

where $V(t)$ is the applied voltage. The perturbation signal $p(t)$ which was fed back to the potentiostat, $V(t)=V_0+Kp(t)$, was calculated by taking the mean value of $h[x_j(t)]$ over every element in the population

$$p(t) = \frac{1}{N}\sum_{j=0}^{N} h[x_j(t)], \tag{33}$$

$$h[x(t)] = \sum_{n=0}^{S} k_n x(t-\tau_n)^n, \tag{34}$$

where K is the overall feedback gain, N is the number of elements in the population, k_n is the nth polynomial feedback coefficient, τ_n is the time delay of the nth polynomial feedback term, and S is the polynomial feedback order.

B. Experimental validation of theory

The synchronization engineering framework, as derived in Sec. IV B for weakly inharmonic waveforms, predicts that nth order feedback can enhance up to and including the nth harmonics of the interaction function for harmonic waveforms, and $(n+1)$th harmonics for weakly inharmonic waveforms. To test the range of the validity of this result, the experimental system was used to measure how the harmonics of an interaction function change with increasing feedback order. The operating voltage of the system was selected to be 1.110 V as this was found to be close enough to the Hopf bifurcation to produce a nearly harmonic waveform, but far enough to ensure that the periodic cycle was robust against external perturbations [Figs. 3(a) and 3(b)].

A two oscillator system was used to measure the interaction function associated with the global feedback signal. This method of measurement was created by extending the work of Miyazaki and Kinoshita[28] to rhythmic systems under global feedback. By measuring the change in the period of the two elements as a function of their phase difference, the interaction function can be experimentally determined.

While the first order harmonic of the waveform accounts for 71% of its magnitude, this may not be sufficient to allow the $O(\epsilon)$ terms of Eq. (27) to be neglected. Therefore, it is expected that the $(n+1)$ order harmonics of the interaction function will be dominant. Figure 3(c) illustrates the percentage of the cumulative magnitude of the harmonics of $H(\phi)$ as a function of the choice of the highest harmonic component to be considered. The cutoff harmonic is given in terms of the feedback order to allow different orders of feedback to be compared to one another. Applying a first order feedback signal to the experimental system produced an interaction function with a large first order component and a relatively small second order component [Figs. 3(d) and 3(g)]. While the first order harmonic only makes up 82% of $H(\phi)$, the combination of the first and second order harmonics account for 96% of its magnitude. When a second order feedback was used, it substantially reduced the first order harmonic of $H(\phi)$ while increasing the second order harmonic [Figs. 3(e) and 3(h)]. A small increase in the third order harmonic was observed due to anharmonicity. Together, these three components make up ~90% of the overall magnitude of $H(\phi)$. Third order feedback increases the ratio between the third and first order harmonics of $H(\phi)$ when compared to first order feedback (0.126 for third order feedback versus 0.027 for first order feedback). Due to strong second order harmonics in the waveform, nontrivial second and fourth order components were also observed in $H(\phi)$. In this case, the first four components account for ~98% of the overall magnitude of the interaction function. These results indicate that the overall shape of the $H(\phi)$ is largely composed of lth harmonics with $l \leqslant n+1$, where n is the feedback order used to produce the function, in line with theoretical expectations.

While the magnitude of the harmonics of H is controlled by the feedback order and their associated feedback gains $\{k_n\}$, the ratio between the symmetric and antisymmetric components of H is controlled by the feedback delay $\{\tau_n\}$. This indicates that increasing the feedback delay is equivalent to shifting the phase of the corresponding components of the interaction function. To validate this claim experimentally, a series of interaction functions was measured using a two oscillator system with global first order feedback over a range of feedback delay τ_1 from 0.013 to 1 rad/2π.

The base interaction function ($\tau_1=0.013$ rad/2π) is illustrated in Fig. 4(a). As the feedback delay was increased, the interaction function was observed to shift [Fig. 4(b)]. To determine the phase shift of the interaction functions when $\tau_1 > 0.013$ rad/2π, a correlation function was calculated between the base interaction function and each of the shifted interaction functions. The correlation function was determined by finding the correlation coefficient between the shifted interaction functions and the base interaction function as the phase of the base function was rotated from 0 to 2π. The phase which produced the maximum value of the correlation coefficient was taken as the experimentally observed phase shift. Figure 4(c) indicates that the phase shift of H is directly proportional to the feedback delay with a proportionality constant of 1. For each measurement, the maximum value of the correlation coefficients remained high (>0.98), indicating that the overall shape of the interaction function was preserved.

Author complimentary copy. Redistribution subject to AIP license or copyright, see http://cha.aip.org/cha/copyright.jsp

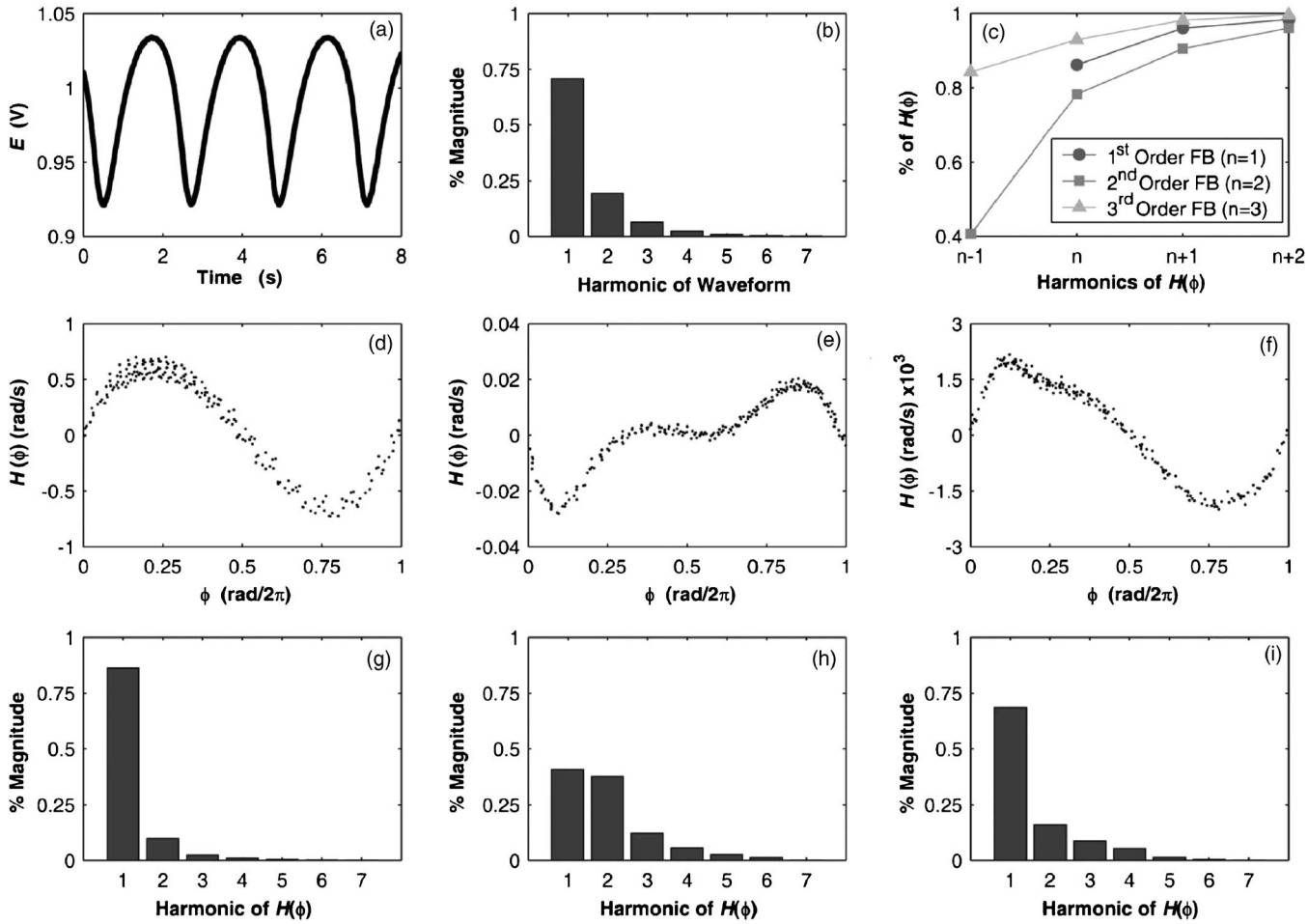

FIG. 3. Electrochemical experiments. (a) Time series of a single nearly smooth oscillator (V_0=1.110 V, R_p=650Ω). (b) Percentage of the first seven harmonics within the waveform of the rhythmic element. (c) The percentage of $H(\phi)$ contained within the first k harmonics of $H(\phi)$ as a function of the choice of k. The values of k have been recentered by the feedback order n. (d–f) Experimental measurements of interaction functions corresponding to (d) first order feedback (K=0.07, k_0=0 V, k_1=1, τ_1=0.013 rad/2π), (e) second order feedback (K=1.6, k_0=−0.003 V, k_1=0, k_2=1 V^{-1}, τ_2=0.013 rad/2π), and (f) third order feedback (K=18, k_0=6.5×10^{-5} V, k_1=0, k_2=0 V^{-1}, k_3=1 V^{-2}, τ_3=0.013 rad/2π). (g–i) Percentage of the first seven harmonic components within the measured interaction function using (g) first order feedback, (h) second order feedback, and (i) third order feedback.

Knowing the relationship between the harmonics of the interaction function and the feedback parameters, it is possible to engineer a feedback that produces a desired interaction function, for example, $H(\phi)=\sin(\phi-\alpha)-r\sin(2\phi)$, where $\alpha=1.32$ and $r=0.25$.

Before the feedback parameters associated with this interaction function can be calculated, the waveform [Fig. 5(a)] and the response function of the oscillations must be determined. The response function was calculated using Eq. (9) from multiple measurements of interaction functions under different feedback conditions (usually first, second, and third order feedback). Since Eq. (9) does not have an analytical solution for the response function, a numerical optimization algorithm was used to calculate the Fourier coefficients of $Z(\phi)$ [Fig. 5(b)]. Once the response function was known, the feedback parameters $\{k_n\}$ and $\{\tau_n\}$ were optimized to achieve

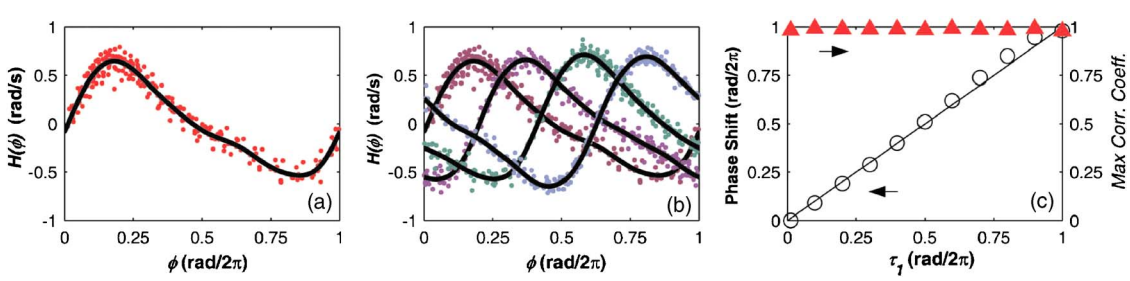

FIG. 4. (Color online) (a) Experimental measurements (dots) with a Fourier fit (line) of an interaction function obtained using linear feedback (V_0 =1.165 V, R_p=650 Ω, K=0.07, k_0=0 V, k_1=1, τ_1=0.013 rad/2π). (b) Interaction functions obtained with τ_1=(0.013,0.2,0.4,0.6) rad/2π respectively. (c) Phase shift of the interaction function and maximum value of the correlation coefficient as a function of feedback delay.

Author complimentary copy. Redistribution subject to AIP license or copyright, see http://cha.aip.org/cha/copyright.jsp

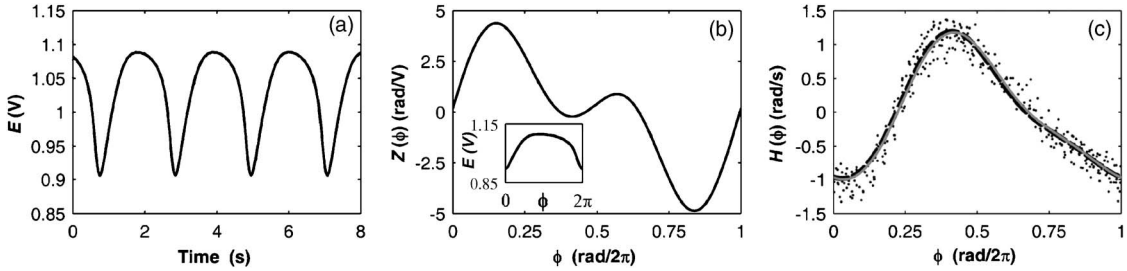

FIG. 5. (a) Time series of electrode potential (V_0=1.165 V, R_p=650 Ω). (b) Response function $Z(\phi)$ and waveform (inset) of a single oscillator. (c) Target (solid line), optimized (dashed line), and measured (dots) interaction function with feedback parameters K=0.0494, k_0=−0.0526 V, k_1=8.7376, k_2=16.3696 V^{-1}, τ_1=0.21 rad/2π, τ_2=0.68 rad/2π.

the desired interaction function also using Eq. (9).[9] The interaction function produced by the optimized feedback parameters was experimentally determined to ensure that they produce the expected function. Figure 5(c) compares the experimentally measured interaction function to the interaction function predicted by Eq. (9). By calculating the Fourier coefficients of the experimental measurements, it was determined that α=1.350 and r=0.242, within 3% of their target values.

C. Phase clustering experiments

To engineer a cluster state in the experimental system, feedback parameters were selected such that the desired cluster state was stabilized. Four sets of experiments were conducted to obtain balanced cluster states composed of one to four clusters, using a population of 64 oscillators. Since a four cluster state requires the presence of fourth order harmonics in the response function, the operation voltage of the system was set at 1.195 V for each experiment causing weakly relaxational oscillations [Figs. 6(a) and 6(b)]. The Fourier coefficients of the waveform and response function can be found in Table III.

As seen in the numerical simulations (Sec. V), there exists a large number of equally valid target interaction functions which can produce the desired cluster states. No specific target function was selected; The Fourier coefficients of the interaction function were optimized such that the desired cluster state was uniquely (or almost uniquely) stabilized. Given previous numerical results, nth order feedback was used to produce an n cluster state. Since linear feedback is sufficient to produce the one cluster state, no optimization was necessary in this case. For the higher order cluster states, a set of penalties were created to describe the fitness of the interaction function based on the distance between its Fourier coefficients and an acceptable range of coefficients. The fitness of $H(\phi)$ was calculated using the equations

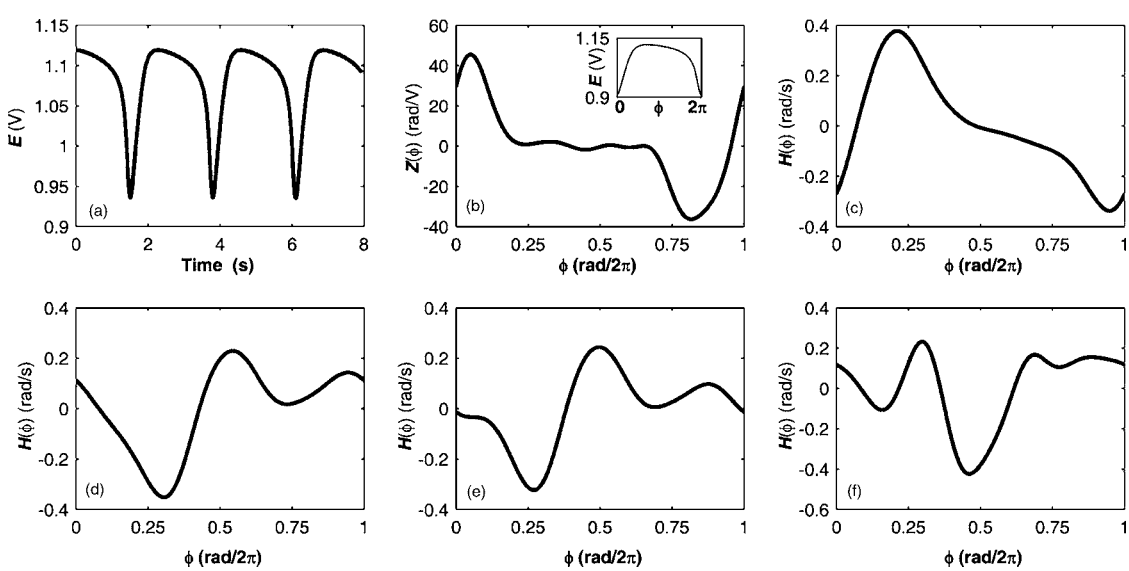

FIG. 6. Experiments: Effects of polynomial feedback on the interaction function. (a) Time series of electrode potential during electrodissolution of nickel wires in sulfuric acid (V_0=1.195 V, R_p=650 Ω). (b) Response function and waveform (inset) of a single oscillator. (c) Interaction function optimized to produce a 1 cluster state (K=0.4, k_0=0 V, k_1=1, τ_1=0.014). (d) Interaction function optimized to produce a 2 cluster state (K=0.0425, k_0=14.97 V, k_1=−3.265, k_2=−66.087 V^{-1}, τ_1=0.014, τ_2=0.368). (e) Interaction function optimized to produce a 3 cluster state (K=0.0424, k_0=20.747 V, k_1=−4.142, k_2=−72.317 V^{-1}, k_3=251.744 V^{-2}, τ_1=0.014 rad/2π, τ_2=0.32, τ_3=0.04). (f) Interaction function optimized to produce a 4 cluster state (K=0.0839, k_0=1.787 V, k_1=−5.099, k_2=−34.136 V^{-1}, k_3=196.145 V^{-2}, k_4=3139.686 V^{-3}, τ_1=0.014, τ_2=0.44, τ_3=0.02, τ_4=0.36). The feedback delay times are given in rad/2π.

Author complimentary copy. Redistribution subject to AIP license or copyright, see http://cha.aip.org/cha/copyright.jsp

TABLE III. (Top) Fourier coefficients of the waveform, response function, and the optimized interaction functions for each of the four experimental objectives. (Bottom) transversal eigenvalues for cluster states 1–4 for each of the four experiments, as calculated from the Fourier coefficients of the corresponding interaction function.

	Waveform		Response Fn		H (1 cluster)		H (2 cluster)		H (3 cluster)		H (4 cluster)	
n	Even	Odd	Even	Odd	Even	Odd	Even	Odd	Even	Odd	Even	Odd
1	−0.0710	+0.0063	+5.6533	+15.460	−0.0799	+0.2211	−0.0014	−0.1688	−0.0619	−0.1289	+0.1503	−0.0617
2	−0.0399	−0.0056	+12.229	+14.496	−0.1303	+0.0819	+0.1475	+0.0446	+0.1313	−0.0157	−0.1384	−0.0291
3	−0.0212	−0.0054	+9.9103	+5.7058	−0.0507	+0.0010	−0.0473	−0.0138	−0.0657	+0.0353	+0.1281	−0.0593
4	−0.0133	−0.0026	+1.8530	+2.6015	−0.0071	+0.0029	−0.0101	−0.0127	−0.0140	−0.0148	−0.0049	+0.0414
5	−0.0064	−0.0005	−0.8616	+2.1364	−0.0004	+0.0031	−0.0067	+0.0013	−0.0009	−0.0057	−0.0275	+0.0069
6	−0.0038	+0.0004	+0.5878	+1.7258	−0.0010	+0.0011	−0.0033	−0.0010	−0.0021	+0.0024	+0.0130	−0.0022

1 cluster	λ_1	λ_2	λ_3	λ_4	2 cluster	λ_1	λ_2	λ_3	λ_4
$M=1$	−0.422	⋯	⋯	⋯	$M=1$	+0.172	⋯	⋯	⋯
$M=2$	+0.058	−0.182	⋯		$M=2$	−0.236	−0.032	⋯	⋯
$M=3$	+0.196	+0.196	−0.010	⋯	$M=3$	−0.014	−0.014	+0.048	⋯
$M=4$	+0.108	+0.159	+0.108	−0.012	$M=4$	−0.051	+0.134	−0.051	+0.051
3 cluster	λ_1	λ_2	λ_3	λ_4	4 cluster	λ_1	λ_2	λ_3	λ_4
$M=1$	+0.127	⋯	⋯	⋯	$M=1$	+0.111	⋯	⋯	⋯
$M=2$	+0.025	+0.076	⋯	⋯	$M=2$	−0.299	−0.094	⋯	⋯
$M=3$	−0.245	−0.245	−0.121	⋯	$M=3$	+0.231	+0.231	+0.191	⋯
$M=4$	+0.034	+0.043	+0.034	+0.059	$M=4$	−0.268	−0.237	−0.268	−0.166

$$\begin{aligned} &\text{fitness} = \text{magnitude} + \text{penalties}, \\ &\text{magnitude} = K\sum_{n=1}^{S}\frac{|k_n|}{10^n}, \\ &\text{penalties} = \sum_{n=1}^{7} P_n, \\ &P_n = \begin{cases} \left|B_n - \dfrac{\text{LB}_n + \text{UB}_n}{2}\right| & \text{for } B_n < \text{LB}_n \text{ or } B_n > \text{UB}_n \\ 0 \quad \text{for } \text{LB}_n < B_n < \text{UB}_n, \end{cases} \end{aligned} \tag{35}$$

where B_i is the ith odd Fourier coefficient of $H(\phi)$. The upper and lower bounds (UB and LB) of the odd Fourier coefficients were selected such that the desired cluster state would be stable and the other (up to 6) cluster states in the system would be unstable. As previously demonstrated, this requires that the interaction function for an n cluster state has a large positive nth order harmonic, and sufficiently negative mth harmonics ($m \neq n$) to destabilize all other cluster states. The target Fourier coefficient ranges reflect this requirement, and are tabulated in Table IV. Additionally, a magnitude adjustment was added to penalize parameter sets which produced a large amplitude feedback signal. Large feedback perturbations are not desirable since they may change the amplitude of the rhythmic elements of the system, violating the phase approximation. By minimizing the value of the fitness variable, the optimization forced the interaction function to have Fourier coefficients necessary to produce the desired cluster state. The optimized interaction functions are illustrated in Figs. 6(c)–6(f).

The transversal eigenvalues of states with one to four clusters can be seen in Table III for each experiment. They were calculated from the Fourier coefficients of the experimental interaction functions using Eqs. (A3) and (A4). The eigenvalues indicate that the desired one, two, and three cluster states are uniquely stable. In the case of the four cluster experiment, the numerical optimization was unable to find feedback parameters to stabilize the four cluster state without also stabilizing the two cluster state. This is not unexpected, given that the difficulty of the optimization dramatically increases with feedback order. Therefore, the four cluster experiment will have a bistability between the four cluster state

TABLE IV. Range of the odd Fourier coefficients of $H(\phi)$ used to optimize feedback parameters to produce phase cluster states 2–4.

Harmonic:	1st	2nd	3rd	4th	5th	6th	7th
2 cluster exp. lower bounds (LB)	−1.0	0.5	−2.0	−0.8	−0.5	−0.50	−0.50
2 cluster exp. upper bounds (UB)	−0.5	1.0	−0.4	−0.3	−0.1	−0.05	−0.05
3 cluster exp. lower bounds (LB)	−1.0	−2.0	0.5	−0.8	−0.5	−0.50	−0.50
3 cluster exp. upper bounds (UB)	−0.5	−0.4	1.0	−0.3	−0.1	−0.05	−0.05
4 cluster exp. lower bounds (LB)	−1.0	−2.0	−0.8	0.2	−0.5	−0.50	−0.50
4 cluster exp. upper bounds (UB)	−0.5	−0.4	−0.3	0.5	−0.1	−0.05	−0.05

Author complimentary copy. Redistribution subject to AIP license or copyright, see http://cha.aip.org/cha/copyright.jsp

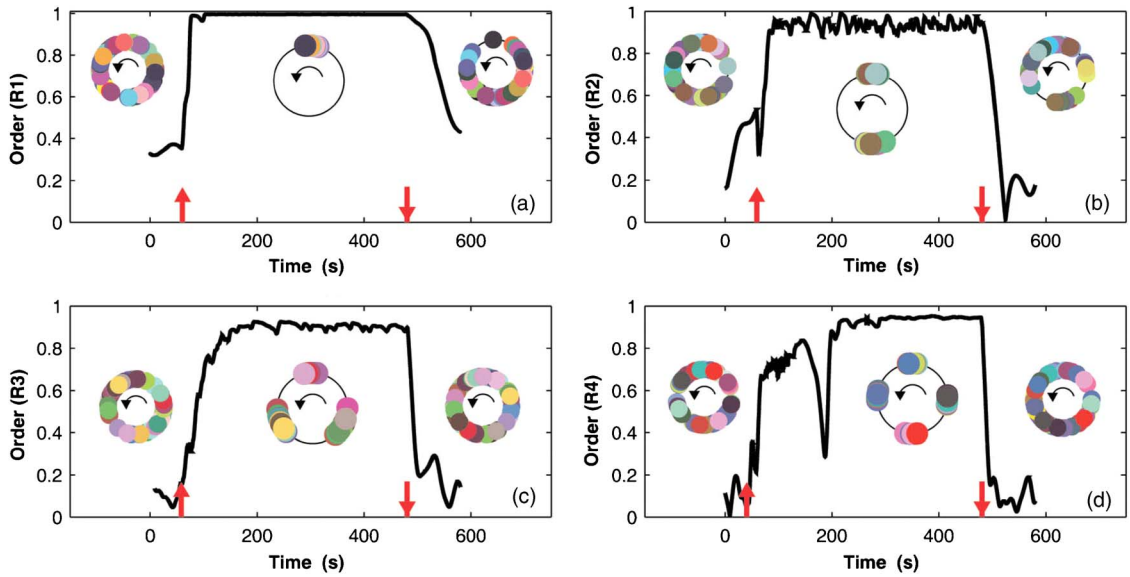

FIG. 7. (Color online) (A) Time series of the R_1 order parameter, using feedback optimized to produce a one cluster state. Arrows indicate the application and termination of the feedback signal. (B) Time series of the R_2 order parameter using feedback optimized to produce a two cluster state. (C) Time series of the R_3 order parameter using feedback optimized to produce a three cluster state. (D) Time series of the R_4 order parameter using feedback optimized to produce a four cluster state.

and the two cluster state. In this case, the final state of the system will be determined by the initial conditions of the system.

After the feedback parameters were determined, they were applied to the experimental system, driving it towards the appropriate cluster state (Fig. 7). Initially no feedback is present in the system, and the rhythmic elements were isolated from one another. Without feedback, these elements have a base frequency of 0.5 Hz $\pm$ 5% with phases randomly distributed between 0 and 2π. Upon application of the feedback signal, the system progresses towards the desired cluster state after a short transient period. When the feedback is removed, the system relaxes back to its original unstructured configuration. Each experiment was successful in producing the desired cluster state from the appropriate feedback signal. It is important to note that although the four cluster experiment was predicted to have a bistability between the two and four cluster states, only the four cluster state was experientially observed. This seems to indicate that the basin of attraction for the four cluster state is sufficiently larger than the basin of the two cluster state.

VII. CONCLUDING REMARKS

We have presented a framework for engineering target dynamical behavior in populations of oscillators with mild feedback. Using a time delayed, nonlinear feedback, Eq. (5), a variety of collective dynamics possible in weakly coupled oscillators can be engineered. The comprehensive theory, based on phase models, behind the methodology has been presented. We have verified the theoretical arguments by both numerical and experimental studies, showing that the methodology can be applied accurately to limit-cycle oscillator systems. As an illustration, by introducing the global feedback given as Eq. (4), various clustering behaviors have been demonstrated numerically and experimentally.

Our methodology is based on the fact that the existence and stability conditions of dynamical states in weakly coupled identical oscillators are characterized by the phase interaction function. Thus, knowing an interaction function resulting in a target collective dynamics, the only remaining issue is how to construct the physical interaction yielding the phase interaction function. An interaction function can be constructed using the proposed feedback function, Eq. (5). The choice of the specific form of the feedback function was motivated by the flexible application of the imposed interaction function for synchronization engineering (Sec. IV). It has been shown that the nth order term of the feedback signal effectively enhances the nth Fourier components of the interaction function. The time delay of the nth term is utilized to arbitrarily tune the balance of even and odd parts of the Fourier components. These correspondences appear intuitively reasonable, as the nth power of the harmonic signal makes a component of harmonic signal having n times frequency and the time delay shifts the waveform. In general, the higher order harmonics in the interaction function are responsible for complex dynamical behavior including dynamical clustering. Our methodology provides a framework for tuning all the harmonics in the interaction function.

A major advantage of our methodology is that the feedback resulting in a target interaction function can be designed through the knowledge of the macroscopic observables of an isolated oscillator, that is, the waveform and the phase response function. When focusing on engineering synchronization properties, a microscopic investigation of the system is not needed. This point is beneficial when applications to biological systems are considered. It is usually a formidable task to construct an appropriate, detailed mathematical model of a biological system. However, the investigation of the phase response function is often possible; the PRCs of circadian oscillators with respect to light or tem-

Author complimentary copy. Redistribution subject to AIP license or copyright, see http://cha.aip.org/cha/copyright.jsp

perature stimuli have been extensively measured[29] as well as the PRCs of neurons with respect to electric stimuli.[21,23]

Our methodology may be used not only to induce dynamical order but also to destroy synchronization. In a previous paper,[9] we have demonstrated that a theoretically designed feedback successfully desynchronizes a population of chemical oscillators which otherwise shows simple synchronization due to global interaction among elements. The model-engineered feedback may find an application in pacemaker and antipacemaker design for medical use (tremors, epilepsy).

Because of the robustness of phase description of limit-cycle oscillators, our methodology for designing interaction function with feedback is robust against (at least weak) noise. However, when a complex dynamical structure is designed, we need to consider the (structural) stability of the designed dynamical behavior in the presence of noise. For example, global noise can enhance the extent of phase synchronization,[30] but can destroy subtle structures like slow switching.[18,19] Therefore, the precision of the fitted interaction function and the overall gain shall be carefully chosen in the presence of noise to obtain the desired structure. Because the proposed methodology was shown to work in the experimental system, our method should be applicable in systems with weak noise and well-defined oscillator waveform and response function.

Limitations to our approach should be noted. We have focused on mild engineering, mild such that essential dynamical properties of elements are preserved. This strategy allows us to use the phase model. The phase models cannot be used with strong feedback because of amplitude effects. Also, the applicability of our method to chaotic oscillators is unclear because the rigorous phase description for chaotic oscillators has not been established yet. In coupled chaotic oscillators, various types of collective behavior arise and some of them are analogous to those in weakly coupled limit-cycle oscillators, such as phase synchronization.[31,32] It would be thus worth trying to extend the method to chaotic oscillators. Another issue arises in cases where limit-cycle oscillators have inherent complex interactions. In the present paper, oscillators are assumed to be independent (i.e., uncoupled) unless feedback is applied. In the presence of inherent global coupling, we have shown the desynchronization is possible using our methodology.[9] What happens if the oscillators are coupled via space dependent interactions or complex networks? This issue requires further exploration, for example, in chemical reaction-diffusion systems and control neural networks.

ACKNOWLEDGMENTS

We thank Alexander Mikhailov, Yoshiki Kuramoto, Ichiro Tsuda, and Yasumasa Nishiura for useful discussions and warm hospitality.

H.K. acknowledges financial support from the Alexander von Humboldt Foundation and the 21st Century COE Program "Mathematics of nonlinear structures via singularities" at Hokkaido University, Japan. This work was supported in part by the National Science Foundation under Grant No. CBET-0730597.

APPENDIX: EXISTENCE AND STABILITY OF THE BALANCED CLUSTER STATES

The balanced n cluster state may be described as

$$\phi_{j\in C_k} = \Omega t + 2k\pi/n, \tag{A1}$$

where the set C_k identifies the oscillators forming the cluster k $(k=0,\ldots,n-1)$ and each set includes N/n elements. Such a solution always exists in the phase model (3). Substituting Eq. (A1) into Eq. (3), we obtain

$$\Omega = \frac{K}{n}\sum_{k=0}^{n-1} H(2k\pi/n) = H_0 + 2\sum_{l=1}^{\infty} \mathrm{Re}\, H_l. \tag{A2}$$

The linear stability problem for the balanced cluster states has been studied by Okuda.[17] The eigenvalues were found to be

$$\lambda_{\mathrm{intra}}^{(n)} = -2\sum_{l=1}^{\infty} l\, \mathrm{Im}\, H_{nl}, \tag{A3}$$

$$\mathrm{Re}\, \lambda_{\mathrm{inter},p} = \lambda_{\mathrm{intra}}^{(n)} - \sum_{l=1}^{\infty} l\, \mathrm{Im}[H_{n(l-1)+p} + H_{nl-p}], \tag{A4}$$

$$\lambda_0 = 0, \tag{A5}$$

where $\lambda_{\mathrm{intra}}^{(n)}$ is associated with intracluster fluctuations ($N-n$ multiplicity), $\lambda_{\mathrm{inter},p}$ $(p=1,\ldots,n-1)$ are associated with intercluster fluctuations, and λ_0 is associated with the identical phase shift.

For the interaction function with $\mathrm{Im}\, H_n > 0$ and $\mathrm{Im}\, H_l \leqslant 0$ for $l \neq n$, the following relation holds:

$$\mathrm{Re}\, \lambda_{\mathrm{inter},p} < \lambda_{\mathrm{intra}}^{(n)} \equiv \lambda_{\mathrm{max}}^{(n)}. \tag{A6}$$

Thus, the n cluster state is linearly stable if and only if $\lambda_{\mathrm{max}}^{(n)} < 0$.

[1] A. T. Winfree, *The Geometry of Biological Time* (Springer, New York, 1980).
[2] P. A. Tass, *Phase Resetting in Medicine and Biology: Stochastic Modeling and Data Analysis* (Springer, Berlin, 1999).
[3] T. Carroll, J. Heagy, and L. Pecora, Phys. Rev. E **54**, 4676 (1996).
[4] B. Blasius, A. Huppert, and L. Stone, Nature (London) **399**, 6734 (1999).
[5] Y. Kuramoto, *Chemical Oscillations, Waves, and Turbulence* (Springer, New York, 1984).
[6] G. Ertl, Science **254**, 1750 (1991).
[7] I. R. Epstein and J. A. Pojman, *Chemical Dynamics: Oscillations, Waves, Patterns, and Chaos* (Oxford University Press, Oxford, 1998).
[8] A. S. Mikhailov and K. Showalter, Phys. Rep. **425**, 79 (2006).
[9] I. Z. Kiss, C. G. Rusin, H. Kori, and J. L. Hudson, Science **316**, 1886 (2007).
[10] Z. Neda, E. Ravasz, Y. Brechet, T. Vicsek, and A. Barabasi, Nature (London) **403**, 849 (2000).
[11] S. M. Reppert and D. R. Weaver, Nature (London) **418**, 935 (2002).
[12] S. H. Strogatz, D. M. Abrams, A. McRobie, B. Eckhardt, and E. Ott, Nature (London) **438**, 43 (2005).
[13] V. K. Vanag, L. Yang, M. Dolnik, A. M. Zhabotinsky, and I. R. Epstein, Nature (London) **406**, 389 (2000).
[14] M. Kim, M. Bertram, M. Pollman, A. von Oertzen, A. S. Mikhailov, H. H. Rotermund, and G. Ertl, Science **292**, 1357 (2001).
[15] S. C. Manrubia, A. S. Mikhailov, and D. H. Zanette, *Emergence of Dynamical Order: Synchronization Phenomena in Complex Systems* (World Scientific, Singapore, 2004).
[16] D. J. Christini and L. Glass, Chaos **12**, 732 (2002).

Author complimentary copy. Redistribution subject to AIP license or copyright, see http://cha.aip.org/cha/copyright.jsp

[17]K. Okuda, Physica D **63**, 424 (1993).
[18]D. Hansel, G. Mato, and C. Meunier, Phys. Rev. E **48**, 347 (1993).
[19]H. Kori and Y. Kuramoto, Phys. Rev. E **63**, 046214 (2001).
[20]H. Kori, Phys. Rev. E **68**, 021919 (2003).
[21]R. F. Galan, G. B. Ermentrout, and N. N. Urban, Phys. Rev. Lett. **94**, 158101 (2005).
[22]I. Z. Kiss, Y. M. Zhai, and J. L. Hudson, Phys. Rev. Lett. **94**, 248301 (2005).
[23]Y. Tsubo, M. Takada, A. Reyes, and T. Fukai, Eur. J. Neurosci. **25**, 3429 (2007).
[24]E. M. Izhikevich, *Dynamical Systems in Neuroscience: The Geometry of Excitability and Bursting* (MIT Press, Cambridge, 2007).
[25]E. M. Izhikevich, Phys. Rev. E **58**, 905 (1998).
[26]P. Glansdorff and I. Prigogine, *Thermodynamic Theory of Structure, Stability, and Fluctuations* (Wiley, London, 1971).
[27]D. Golomb, D. Hansel, B. Shraiman, and H. Y. Sompolinsky, Phys. Rev. A **45**, 3516 (1992).
[28]J. Miyazaki and S. Kinoshita, Phys. Rev. Lett. **96**, 194101 (2006).
[29]C. H. Johnson, Chronobiol Int. **16**, 711 (1999).
[30]C. Zhou, J. Kurths, I. Kiss, and J. Hudson, Phys. Rev. Lett. **89**, 014101 (2002).
[31]S. Boccaletti, J. Kurths, G. Osipov, D. Valladares, and C. Zhou, Phys. Rep. **366**, 1 (2002).
[32]A. Pikovsky, M. Rosenblum, and J. Kurths, *Synchronization: A Universal Concept of Nonlinear Sciences* (Cambridge University Press, Cambridge, 2001).

Author complimentary copy. Redistribution subject to AIP license or copyright, see http://cha.aip.org/cha/copyright.jsp